

## First Observation of the Decay $B^0 \rightarrow D^{*+} D^{*-}$

M. Artuso,<sup>1</sup> E. Dambasuren,<sup>1</sup> S. Kopp,<sup>1</sup> G. C. Moneti,<sup>1</sup> R. Mountain,<sup>1</sup> S. Schuh,<sup>1</sup> T. Skwarnicki,<sup>1</sup> S. Stone,<sup>1</sup> A. Titov,<sup>1</sup> G. Viehhauser,<sup>1</sup> J. C. Wang,<sup>1</sup> S. E. Csorna,<sup>2</sup> K. W. McLean,<sup>2</sup> S. Marka,<sup>2</sup> Z. Xu,<sup>2</sup> R. Godang,<sup>3</sup> K. Kinoshita,<sup>3,\*</sup> I. C. Lai,<sup>3</sup> P. Pomianowski,<sup>3</sup> S. Schrenk,<sup>3</sup> G. Bonvicini,<sup>4</sup> D. Cinabro,<sup>4</sup> R. Greene,<sup>4</sup> L. P. Perera,<sup>4</sup> G. J. Zhou,<sup>4</sup> S. Chan,<sup>5</sup> G. Eigen,<sup>5</sup> E. Lipeles,<sup>5</sup> J. S. Miller,<sup>5</sup> M. Schmidtler,<sup>5</sup> A. Shapiro,<sup>5</sup> W. M. Sun,<sup>5</sup> J. Urheim,<sup>5</sup> A. J. Weinstein,<sup>5</sup> F. Würthwein,<sup>5</sup> D. E. Jaffe,<sup>6</sup> G. Masek,<sup>6</sup> H. P. Paar,<sup>6</sup> E. M. Potter,<sup>6</sup> S. Prell,<sup>6</sup> V. Sharma,<sup>6</sup> D. M. Asner,<sup>7</sup> A. Eppich,<sup>7</sup> J. Gronberg,<sup>7</sup> T. S. Hill,<sup>7</sup> C. M. Korte,<sup>7</sup> D. J. Lange,<sup>7</sup> R. J. Morrison,<sup>7</sup> H. N. Nelson,<sup>7</sup> T. K. Nelson,<sup>7</sup> D. Roberts,<sup>7</sup> H. Tajima,<sup>7</sup> B. H. Behrens,<sup>8</sup> W. T. Ford,<sup>8</sup> A. Gritsan,<sup>8</sup> H. Krieg,<sup>8</sup> J. Roy,<sup>8</sup> J. G. Smith,<sup>8</sup> J. P. Alexander,<sup>9</sup> R. Baker,<sup>9</sup> C. Bebek,<sup>9</sup> B. E. Berger,<sup>9</sup> K. Berkelman,<sup>9</sup> V. Boisvert,<sup>9</sup> D. G. Cassel,<sup>9</sup> D. S. Crowcroft,<sup>9</sup> M. Dickson,<sup>9</sup> S. von Dombrowski,<sup>9</sup> P. S. Drell,<sup>9</sup> K. M. Ecklund,<sup>9</sup> R. Ehrlich,<sup>9</sup> A. D. Foland,<sup>9</sup> P. Gaidarev,<sup>9</sup> L. Gibbons,<sup>9</sup> B. Gittelman,<sup>9</sup> S. W. Gray,<sup>9</sup> D. L. Hartill,<sup>9</sup> B. K. Heltsley,<sup>9</sup> P. I. Hopman,<sup>9</sup> J. Kandaswamy,<sup>9</sup> N. Katayama,<sup>9</sup> D. L. Kreinick,<sup>9</sup> T. Lee,<sup>9</sup> Y. Liu,<sup>9</sup> N. B. Mistry,<sup>9</sup> C. R. Ng,<sup>9</sup> E. Nordberg,<sup>9</sup> M. Ogg,<sup>9,†</sup> J. R. Patterson,<sup>9</sup> D. Peterson,<sup>9</sup> D. Riley,<sup>9</sup> A. Soffer,<sup>9</sup> B. Valant-Spaight,<sup>9</sup> A. Warburton,<sup>9</sup> C. Ward,<sup>9</sup> M. Athanas,<sup>10</sup> P. Avery,<sup>10</sup> C. D. Jones,<sup>10</sup> M. Lohner,<sup>10</sup> C. Prescott,<sup>10</sup> A. I. Rubiera,<sup>10</sup> J. Yelton,<sup>10</sup> J. Zheng,<sup>10</sup> G. Brandenburg,<sup>11</sup> R. A. Briere,<sup>11</sup> A. Ershov,<sup>11</sup> Y. S. Gao,<sup>11</sup> D. Y.-J. Kim,<sup>11</sup> R. Wilson,<sup>11</sup> T. E. Browder,<sup>12</sup> Y. Li,<sup>12</sup> J. L. Rodriguez,<sup>12</sup> H. Yamamoto,<sup>12</sup> T. Bergfeld,<sup>13</sup> B. I. Eisenstein,<sup>13</sup> J. Ernst,<sup>13</sup> G. E. Gladding,<sup>13</sup> G. D. Gollin,<sup>13</sup> R. M. Hans,<sup>13</sup> E. Johnson,<sup>13</sup> I. Karliner,<sup>13</sup> M. A. Marsh,<sup>13</sup> M. Palmer,<sup>13</sup> M. Selen,<sup>13</sup> J. J. Thaler,<sup>13</sup> K. W. Edwards,<sup>14</sup> A. Bellerive,<sup>15</sup> R. Janicek,<sup>15</sup> P. M. Patel,<sup>15</sup> A. J. Sadoff,<sup>16</sup> R. Ammar,<sup>17</sup> P. Baringer,<sup>17</sup> A. Bean,<sup>17</sup> D. Besson,<sup>17</sup> D. Coppage,<sup>17</sup> R. Davis,<sup>17</sup> S. Kotov,<sup>17</sup> I. Kravchenko,<sup>17</sup> N. Kwak,<sup>17</sup> L. Zhou,<sup>17</sup> S. Anderson,<sup>18</sup> Y. Kubota,<sup>18</sup> S. J. Lee,<sup>18</sup> R. Mahapatra,<sup>18</sup> J. J. O'Neill,<sup>18</sup> R. Poling,<sup>18</sup> T. Riehle,<sup>18</sup> A. Smith,<sup>18</sup> M. S. Alam,<sup>19</sup> S. B. Athar,<sup>19</sup> Z. Ling,<sup>19</sup> A. H. Mahmood,<sup>19</sup> S. Timm,<sup>19</sup> F. Wappler,<sup>19</sup> A. Anastassov,<sup>20</sup> J. E. Duboscq,<sup>20</sup> K. K. Gan,<sup>20</sup> C. Gwon,<sup>20</sup> T. Hart,<sup>20</sup> K. Honscheid,<sup>20</sup> H. Kagan,<sup>20</sup> R. Kass,<sup>20</sup> J. Lee,<sup>20</sup> J. Lorenc,<sup>20</sup> H. Schwarthoff,<sup>20</sup> A. Wolf,<sup>20</sup> M. M. Zoeller,<sup>20</sup> S. J. Richichi,<sup>21</sup> H. Severini,<sup>21</sup> P. Skubic,<sup>21</sup> A. Undrus,<sup>21</sup> M. Bishai,<sup>22</sup> S. Chen,<sup>22</sup> J. Fast,<sup>22</sup> J. W. Hinson,<sup>22</sup> N. Menon,<sup>22</sup> D. H. Miller,<sup>22</sup> E. I. Shibata,<sup>22</sup> I. P. J. Shipsey,<sup>22</sup> S. Glenn,<sup>23</sup> Y. Kwon,<sup>23,‡</sup> A. L. Lyon,<sup>23</sup> S. Roberts,<sup>23</sup> E. H. Thorndike,<sup>23</sup> C. P. Jessop,<sup>24</sup> K. Lingel,<sup>24</sup> H. Marsiske,<sup>24</sup> M. L. Perl,<sup>24</sup> V. Savinov,<sup>24</sup> D. Ugolini,<sup>24</sup> X. Zhou,<sup>24</sup> T. E. Coan,<sup>25</sup> V. Fadeyev,<sup>25</sup> I. Korolkov,<sup>25</sup> Y. Maravin,<sup>25</sup> I. Narsky,<sup>25</sup> R. Stroynowski,<sup>25</sup> J. Ye,<sup>25</sup> and T. Wlodek<sup>25</sup>

(CLEO Collaboration)

<sup>1</sup>Syracuse University, Syracuse, New York 13244

<sup>2</sup>Vanderbilt University, Nashville, Tennessee 37235

<sup>3</sup>Virginia Polytechnic Institute and State University, Blacksburg, Virginia 24061

<sup>4</sup>Wayne State University, Detroit, Michigan 48202

<sup>5</sup>California Institute of Technology, Pasadena, California 91125

<sup>6</sup>University of California, San Diego, La Jolla, California 92093

<sup>7</sup>University of California, Santa Barbara, California 93106

<sup>8</sup>University of Colorado, Boulder, Colorado 80309-0390

<sup>9</sup>Cornell University, Ithaca, New York 14853

<sup>10</sup>University of Florida, Gainesville, Florida 32611

<sup>11</sup>Harvard University, Cambridge, Massachusetts 02138

<sup>12</sup>University of Hawaii at Manoa, Honolulu, Hawaii 96822

<sup>13</sup>University of Illinois, Urbana-Champaign, Illinois 61801

<sup>14</sup>Carleton University, Ottawa, Ontario, Canada K1S 5B6  
and the Institute of Particle Physics, Canada

<sup>15</sup>McGill University, Montréal, Québec, Canada H3A 2T8  
and the Institute of Particle Physics, Canada

<sup>16</sup>Ithaca College, Ithaca, New York 14850

<sup>17</sup>University of Kansas, Lawrence, Kansas 66045

<sup>18</sup>University of Minnesota, Minneapolis, Minnesota 55455

<sup>19</sup>State University of New York at Albany, Albany, New York 12222

<sup>20</sup>The Ohio State University, Columbus, Ohio 43210

<sup>21</sup>University of Oklahoma, Norman, Oklahoma 73019

<sup>22</sup>Purdue University, West Lafayette, Indiana 47907

<sup>23</sup>University of Rochester, Rochester, New York 14627

<sup>24</sup>Stanford Linear Accelerator, Stanford University, Stanford, California 94309

<sup>25</sup>Southern Methodist University, Dallas, Texas 75275

(Received 16 November 1998)

We have observed four fully reconstructed  $B^0 \rightarrow D^{*+}D^{*-}$  candidates in  $5.8 \times 10^6 Y(4S) \rightarrow B\bar{B}$  decays recorded with the CLEO detector. The background is estimated to be  $0.31 \pm 0.10$  events. The probability that the background could produce four or more signal candidates with the observed distribution among  $D^{*+}$  and  $D^{*-}$  decay modes is  $1.1 \times 10^{-4}$ . The measured decay rate,  $\mathcal{B}(B^0 \rightarrow D^{*+}D^{*-}) = [6.2_{-2.9}^{+4.0}(\text{stat}) \pm 1.0(\text{syst})] \times 10^{-4}$ , is large enough for this decay mode to be of interest for the measurement of a time-dependent CP asymmetry. [S0031-9007(99)08881-X]

PACS numbers: 13.25.Hw, 11.30.Er

The Cabibbo-suppressed decay  $B^0 \rightarrow D^{*+}D^{*-}$  is a promising channel for searches of CP violation in  $B^0$  meson decays at future  $B$  factories [1,2]. Within the framework of the standard model, the proper time-dependent CP asymmetry in the decay  $B^0 \rightarrow D^{*+}D^{*-}$  could provide a measurement of the angle  $\beta$  of the unitarity triangle [3] in the same way as the well-known decay  $B^0 \rightarrow J/\psi K^0$  [1,2]. The final state  $D^{*+}D^{*-}$  may be an admixture of CP-even and CP-odd states which could complicate such a measurement. However, the resulting dilution of the asymmetry is estimated to be small [4], and the two CP components can be disentangled using angular correlations in the final state [5]. The decay amplitude for the process  $B^0 \rightarrow D^{*+}D^{*-}$  is expected to be dominated by the decay  $\bar{b} \rightarrow \bar{c}W^+$ ;  $W^+ \rightarrow c\bar{d}$ . The branching fraction for this process can be estimated from the measured rate [6] of the Cabibbo-favored decay  $B^0 \rightarrow D_s^{*+}D_s^{*-}$  and is  $\mathcal{B}(B^0 \rightarrow D^{*+}D^{*-}) \approx (f_{D^*}/f_{D_s^*})^2 \tan^2\theta_C \mathcal{B}(B^0 \rightarrow D_s^{*+}D_s^{*-}) \approx 0.1\%$ , where the  $f_X$  are the decay constants and  $\theta_C$  is the Cabibbo angle.

The CLEO [7] and ALEPH [8] Collaborations have reported 90% C.L. upper limits on  $\mathcal{B}(B^0 \rightarrow D^{*+}D^{*-})$  of  $22 \times 10^{-4}$  and  $61 \times 10^{-4}$ , respectively. In this Letter we report on the first observation of the decay  $B^0 \rightarrow D^{*+}D^{*-}$  and a measurement of its decay rate. This measurement supersedes the previous CLEO search [7].

The data were recorded at the Cornell Electron Storage Ring (CESR) with two configurations of the CLEO detector, called CLEO II [9] and CLEO II.V. In the CLEO II.V configuration, the innermost wire chamber was replaced with a precision three-layer silicon vertex detector (SVX) [10]. Each layer of the SVX provided precise measurements of the  $\phi$  and  $z$  coordinates of the charged particle trajectory. (The  $z$  axis of the CLEO cylindrical coordinate system is coincident with the  $e^+$  beam direction.) The results in this Letter are based upon an integrated luminosity of  $3.14(2.46) \text{ fb}^{-1}$  of  $e^+e^-$  data recorded at the  $Y(4S)$  energy and  $1.57(1.26) \text{ fb}^{-1}$  recorded 60 MeV below the  $Y(4S)$  energy with the CLEO II (CLEO II.V) configuration. The Monte Carlo simulation of the CLEO detector response was based upon GEANT [11]. Simulated events for the CLEO II and CLEO II.V configurations were processed in the same manner as the data.

Candidates for the decay  $B^0 \rightarrow D^{*+}D^{*-}$  with the subsequent decays  $D^{*+} \rightarrow D^0\pi_s^+$  and  $D^{*-} \rightarrow D^+\pi_s^0$  were selected. The  $D^0$  and  $D^+$  mesons were reconstructed in

the eleven decay modes listed in Table I. In this Letter, “ $D$ ” refers to both  $D^0$  and  $D^+$  mesons, and “ $\pi_s$ ” refers to the slow pion produced in  $D^{*+}$  decay. In addition, reference to charge conjugate states is implicit unless explicitly stated. The charged track candidates from  $D^{*+}$  and  $D$  meson decays were required to originate near the  $e^+e^-$  interaction point. Charged kaons and pions were distinguished using the charged particle’s measured specific ionization ( $dE/dx$ ) and time of flight across the tracking volume. We required that the  $dE/dx$  and time-of-flight information, when available, was consistent within 2.5 (3.0) standard deviations for the charged kaon (pion) daughters of the  $D$  meson candidate. Charged tracks and  $K_S^0$  candidates forming a  $D$  candidate were required to originate from a common vertex. The  $K_S^0$  candidates were selected through their decay into  $\pi^+\pi^-$  mesons. The decay of the  $K_S^0$  candidate was required to be displaced from the  $e^+e^-$  interaction point, and at least one daughter pion was required to be inconsistent with originating at the interaction point. Neutral pions were reconstructed from photon pairs detected in the electromagnetic calorimeter. The photons were required to have an energy of at least 30 (50) MeV in the barrel (end cap) region, and their invariant mass was required to be within 3 standard deviations of the nominal  $\pi^0$  meson mass [3]. The  $\pi^0$  momentum was required to be at least 70 (100) MeV for  $D^{*+}$  ( $D$ ) daughters. To reduce backgrounds, we accepted both  $(D^0\pi_s^+)(\bar{D}^0\pi_s^-)$  and  $(D^0\pi_s^+)(D^-\pi_s^0)$  combinations but not  $(D^+\pi_s^0)(D^-\pi_s^0)$ . A fit constraining the mass of each  $D^{*+}$  candidate to the nominal value [3] improved the  $D^{*+}$  momentum resolution by 14% in simulated events.

TABLE I. The  $D^0$  and  $D^+$  meson decay modes used in this analysis and their branching fractions [3]. The branching fractions  $\mathcal{B}(K_S^0 \rightarrow \pi^+\pi^-)$  and  $\mathcal{B}(\phi \rightarrow K^+K^-)$  are included for the modes containing  $K_S^0$  or  $\phi$  mesons.

$D^0$ Decay modes		$D^+$ Decay modes	
Decay mode	Branching fraction (%)	Decay mode	Branching fraction (%)
$K^-\pi^+$	$3.85 \pm 0.09$	$K^-\pi^+\pi^+$	$9.0 \pm 0.6$
$K^-\pi^+\pi^0$	$13.9 \pm 0.9$	$K_S^0\pi^+$	$1.0 \pm 0.1$
$K^-\pi^+\pi^+\pi^-$	$7.6 \pm 0.4$	$K_S^0\pi^+\pi^0$	$3.3 \pm 1.0$
$K_S^0\pi^+\pi^-$	$1.9 \pm 0.1$	$K_S^0\pi^+\pi^+\pi^-$	$2.4 \pm 0.3$
$K_S^0\pi^+\pi^-\pi^0$	$3.4 \pm 0.4$	$\phi\pi^+$	$0.30 \pm 0.03$
		$\phi\pi^+\pi^0$	$1.1 \pm 0.5$
Total	$30.6 \pm 1.3$	Total	$17.1 \pm 1.6$

The  $B^0 \rightarrow D^{*+}D^{*-}$  candidates were selected by means of four observables. The first observable,  $\chi_M^2$ , measured the deviation of each  $D$  and  $D^{*+}$  candidate from the nominal mass ( $M_i^n$ ) and mass difference ( $\Delta M_i^n$ ), respectively,

$$\chi_M^2 \equiv \sum_{i=1,2} \left[ \left( \frac{M_i - M_i^n}{\sigma(M_i)} \right)^2 + \left( \frac{\Delta M_i - \Delta M_i^n}{\sigma(\Delta M_i)} \right)^2 \right], \quad (1)$$

where  $\sigma(M_i)$  and  $\sigma(\Delta M_i)$  are the average resolutions in the reconstructed  $D$  candidate mass  $M_i$  and the mass difference  $\Delta M_i \equiv M_i(D^{*+}) - M_i$ , respectively, and  $i = 1, 2$  corresponds to the  $D^{*+, -}$  and the  $D, \bar{D}$  daughters. If an event had more than one  $B^0 \rightarrow D^{*+}D^{*-}$  candidate, then the candidate with the lowest  $\chi_M^2$  was chosen. The second observable,  $L/\sigma(L)$ , is the significance of the projected three-dimensional distance  $L$  between the reconstructed  $D$  and  $\bar{D}$  meson decay vertices,

$$L = (\vec{V}_D - \vec{V}_{\bar{D}}) \cdot \frac{(\vec{p}_D - \vec{p}_{\bar{D}})}{|\vec{p}_D - \vec{p}_{\bar{D}}|},$$

where  $\vec{p}_D$  and  $\vec{V}_D$  are the momentum and decay vertex position of the  $D$  candidate, respectively, and  $\sigma(L)$  was calculated from the covariance matrices of the  $D$  and  $\bar{D}$  tracks resulting from the vertex fits of the  $D$  daughters. This observable exploits the relatively long  $D^+$  meson lifetime and the precise decay vertex resolution available in CLEO II.V. The difference between the energy of the  $B^0$  candidate and the beam energy,  $\Delta E \equiv E(D^{*+}) + E(D^{*-}) - E_{\text{beam}}$ , is the third observable. In simulated  $B^0 \rightarrow D^{*+}D^{*-}$  decays, the  $\Delta E$  resolution improves to 8.0 MeV from  $\sim 14$  MeV after applying the  $D^{*+}$  mass constraint. The fourth observable is the beam-constrained  $B^0$  candidate mass  $M_B \equiv \sqrt{E_{\text{beam}}^2 - \vec{p}_B^2}$  where  $\vec{p}_B$  is the momentum of the  $B$  candidate. The resolution of  $M_B$ , dominated by the beam energy spread, was measured to be 2.5 MeV [12].

The selection criteria for these four observables were optimized for signal significance using simulated signal and background events. The optimal criteria determined were  $\chi_M^2 < 10$ ,  $L/\sigma(L) > 0$  for the  $(D^0\pi_s^+)(D^-\pi_s^0)$  candidates in the CLEO II.V data only,  $|\Delta E| < 20$  MeV, and  $|\Delta M_B| \equiv |M_B - M_B^{\text{nom}}| < 6.25$  MeV where  $M_B^{\text{nom}}$  is the nominal  $B^0$  meson mass [3].

With these criteria, the reconstruction efficiency for each  $D^{*+}$  and  $D$  decay channel was measured from simulated  $B^0 \rightarrow D^{*+}D^{*-}$  decays. Important issues in  $B^0 \rightarrow D^{*+}D^{*-}$  reconstruction are the ability to reconstruct the trajectory of charged slow pions  $\pi_s^+$  that populate the momentum range from 60 to 190 MeV and the accurate determination of their reconstruction efficiency. The track-finding algorithm used for these results was optimized for the CLEO II but not the CLEO II.V configuration. As a result, the ratio of the  $D^{*+} \rightarrow D^0\pi_s^+$  reconstruction efficiency in the CLEO II.V data to that in the CLEO II data is  $(65 \pm 6)\%$  due to the reduced  $\pi_s^+$  recon-

struction efficiency. We corrected the  $D^{*+}$  reconstruction efficiency for differences in the inclusive  $D^{*+}$  meson yields between data and simulation in this momentum range using the measured inclusive  $D^{*+}$  production spectrum in  $Y(4S) \rightarrow B\bar{B}$  events [13]. Including the  $D^{*+}$  and  $D$  daughter branching fractions, the overall reconstruction efficiency was  $\mathcal{E} = (10.08 \pm 1.10) \times 10^{-4}$ . An appropriate figure of merit is the single event sensitivity, defined as  $[2N(B\bar{B})f_{00}\mathcal{E}]^{-1}$ , where  $N(B\bar{B})$  is the number of  $B\bar{B}$  pairs and  $f_{00} = 0.48 \pm 0.04$  is the fraction of  $Y(4S)$  decays to  $B^0\bar{B}^0$  [14]. Our sample of  $3.3 \times 10^6$  ( $2.5 \times 10^6$ )  $B\bar{B}$  pairs in the CLEO II (CLEO II.V) data gives a single event sensitivity for  $B^0 \rightarrow D^{*+}D^{*-}$  of  $(1.8 \pm 0.3) \times 10^{-4}$ .

We used two independent methods to estimate the contributions of the background to the signal region, defined as  $|\Delta E| < 20$  MeV and  $|\Delta M_B| < 6.25$  MeV. In method 1, we scaled the number of candidates in a grand sideband (GSB) to estimate the background contribution to the signal region. The GSB is defined as the region  $|\Delta E| < 400$  MeV and  $5.20 < M_B < 5.29$  GeV excluding the region  $|\Delta E| < 50$  MeV and  $5.26 < M_B < 5.29$  GeV and is indicated in Fig. 1(a). The scale factor for the GSB events is the ratio of the area of the signal region to that of the GSB. The estimated background contribution to the signal region is  $0.261 \pm 0.043$  events from method 1. In principle, the background contribution determined from the GSB slightly overestimates the actual background due to  $B \rightarrow D^{*+}D^{*-}X_{s,d}$  decays that are kinematically forbidden to populate the signal region but may be present in the  $\Delta E$  or  $M_B$  sideband regions. This overestimation is negligible as discussed below.

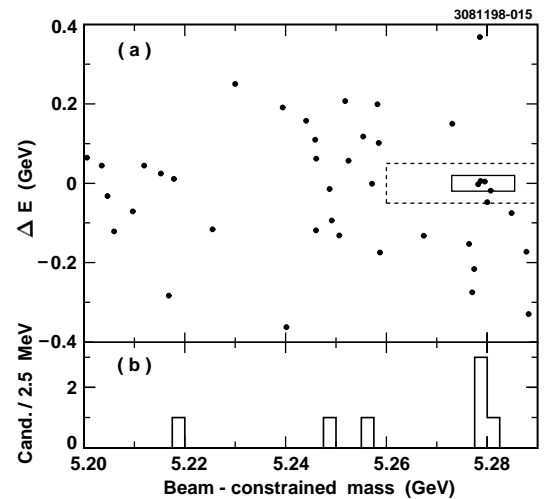


FIG. 1. (a) The  $\Delta E$  vs the beam-constrained mass distribution for all  $B^0 \rightarrow D^{*+}D^{*-}$  candidates in the data taken on the  $Y(4S)$  resonance. The signal region is indicated by the box with the solid line. The area outside the dashed line is the grand sideband (GSB). There are four candidates in the signal region and a total of 41 candidates in the entire distribution. (b) The beam-constrained mass distribution for  $B^0 \rightarrow D^{*+}D^{*-}$  candidates satisfying  $|\Delta E| < 20$  MeV.

For method 2, we decomposed the background into four classes and estimated the contribution of each class separately. The dominant background class is composed of random combinations of  $D^{*+}$  and  $D^{*-}$  candidates in which either one or both candidates is “fake”; that is, they are not composed of the daughters of an actual  $D^{*+}$  decay. The other background classes comprise combinations in which the  $D^{*+}$  and  $D^{*-}$  candidates arise from actual  $D^{*+}$  and  $D^{*-}$  meson decays that are roughly back-to-back. The contributing processes are (1)  $e^+e^- \rightarrow c\bar{c}$  with  $c \rightarrow D^{*+}$  and  $\bar{c} \rightarrow D^{*-}$ , (2)  $Y(4S) \rightarrow B\bar{B}$  with  $B \rightarrow D^{*+}X$  and  $\bar{B} \rightarrow D^{*-}Y$ , and (3)  $B \rightarrow D^{*+}D^{*-}X_{s,d}$  where  $X_{s,d}$  represents either a strange or nonstrange meson from the decay of an orbitally or a radially excited  $D$  meson or nonresonant  $D^{*+}X$  production.

We estimated the combinatorial background from data with explicit fake  $D^{*+}$  candidates formed by replacing  $M_1^n$  in  $\chi_M^2$  in Eq. (1) with  $M_1^n + 6\sigma(M_1)$  or  $M_1^n - 6\sigma(M_1)$ . We first formed a sample of fake  $D^{*+}$  candidates combined with standard  $D^{*-}$  candidates. Similarly, we formed a sample of fake  $D^{*+}$  candidates combined with fake  $D^{*-}$  candidates. The combinatorial background can be derived from these samples and contributes an estimated  $0.304 \pm 0.040$  events when scaled to the signal region.

The contribution of the process (1)  $e^+e^- \rightarrow c\bar{c}$ ,  $c \rightarrow D^{*+}$ ,  $\bar{c} \rightarrow D^{*-}$  was estimated from the data taken 60 MeV below the  $Y(4S)$  after subtracting the combinatorial background using the method described above. The estimated number of events in the signal region from this process was  $0.039 \pm 0.030$  after correction for the relative cross section and luminosity.

The contribution of processes (2) and (3) from  $Y(4S) \rightarrow B\bar{B}$  were estimated from a sample of simulated events approximately 10 times the data sample. The process (2)  $Y(4S) \rightarrow B\bar{B}$ ,  $B \rightarrow D^{*+}X$ ,  $\bar{B} \rightarrow D^{*-}X$  was estimated to

contribute  $0.024 \pm 0.003$  events to the signal region. The contributions of  $B \rightarrow D^{*+}D^{*-}X_{s,d}$  were determined to be negligible assuming  $\mathcal{B}(B \rightarrow D^{*+}D^{*-}X_s) = 1.8\%$  [15] and  $\mathcal{B}(B \rightarrow D^{*+}D^{*-}X_d) \approx \mathcal{B}(B^0 \rightarrow D^{*+}D^{*-})$ . The estimated contribution to the signal region from the sum of all backgrounds is  $0.367 \pm 0.051$  events for method 2.

The background rates obtained from these two statistically independent methods were averaged to yield the estimated background contribution to the signal region of  $0.306 \pm 0.033(\text{stat}) \pm 0.094(\text{syst})$ . The 31% systematic uncertainty arises from the uncertainty in the shapes of the  $\Delta E$  and  $M_B$  distributions of the background. The systematic uncertainty was taken to be the difference in the scale factor when these distributions were fitted with second- and first-order polynomials, respectively, instead of a zeroth-order polynomial.

The distribution of the 41 candidates passing the selection criteria in the  $Y(4S)$  data sample in the  $\Delta E$  vs  $M_B$  plane is shown in Fig. 1. There are four candidates in the signal region. The observed number of candidates and the estimated background for the  $(D^0\pi_s^+)(\bar{D}^0\pi_s^-)$  and  $(D^0\pi_s^+)(D^-\pi_s^0)$  submodes are listed in Table II. Also listed in Table II is the probability that a fluctuation of the estimated background could produce the observed number of signal candidates or more in each submode. The calculation of the background fluctuation probability assumes that the statistical uncertainty in the background in the two submodes is uncorrelated and that the systematic uncertainty in the background is fully correlated between the submodes. Integrating over all background levels, assuming that the number of background events is normally distributed about its central value for each submode [16], we find that the combined probability that the estimated background could produce the observed number of signal candidates or more in the two submodes is  $1.1 \times 10^{-4}$ .

TABLE II. The efficiency, observed number of candidates, and estimated number of background events in the  $(D^0\pi_s^+)(\bar{D}^0\pi_s^-)$  and  $(D^0\pi_s^+)(D^-\pi_s^0)$  decay submodes. The reconstruction efficiency  $\mathcal{E}$  includes the  $D$  and  $D^{*+}$  daughter branching fractions. The row labeled “all  $(\Delta E, M_B)$ ” is the total number of  $B^0 \rightarrow D^{*+}D^{*-}$  candidates in each submode in the  $5.20 < M(B) < 5.29$  GeV and  $|\Delta E| < 400$  MeV region. The row labeled “Signal region” contains the observed number of signal candidates in the  $|\Delta E| < 20$  MeV and  $|\Delta M_B| < 6.25$  MeV region. “Bkg. meth. 1” and “Bkg. meth. 2” are the number of background events in the signal region estimated using the two independent methods described in the text. The sixth row contains the average estimated number of background events in the signal region. Only statistical uncertainties are included for the upper six rows. The calculation of the background fluctuation probability  $\mathbf{P}$  is described in the text.

	$(D^0\pi_s^+)$ $(\bar{D}^0\pi_s^-)$	$(D^0\pi_s^+)$ $(D^-\pi_s^0)$	Total
$\mathcal{E} \times 10^4$	$6.06 \pm 1.02$	$4.02 \pm 0.40$	$10.08 \pm 1.10$
All $(\Delta E, M_B)$	13	28	41
Signal region	2	2	4
Bkg. meth. 1	$0.080 \pm 0.024$	$0.181 \pm 0.036$	$0.261 \pm 0.043$
Bkg. meth. 2	$0.091 \pm 0.024$	$0.275 \pm 0.044$	$0.367 \pm 0.051$
Average Bkg.	$0.085 \pm 0.017$	$0.219 \pm 0.028$	$0.306 \pm 0.033$
$\mathbf{P}$	$3.85 \times 10^{-3}$	$2.24 \times 10^{-2}$	$1.10 \times 10^{-4}$

The branching fraction of  $B^0 \rightarrow D^{*+}D^{*-}$  was calculated using a maximum likelihood technique that took into account the signal efficiency and estimated background contribution for each  $D$  decay mode in the CLEO II and CLEO II.V data samples. The branching fraction was determined to be  $\mathcal{B}(B^0 \rightarrow D^{*+}D^{*-}) = (6.2_{-2.9}^{+4.0} \pm 1.0) \times 10^{-4}$ , where the first error is statistical and the second is systematic. The systematic uncertainty is dominated by the uncertainties in  $\mathcal{E}$  (13.3%) and  $f_{00}$  (8.3%). The product branching function, using the  $D^{*+}$  and  $D$  decay modes as in this Letter,  $\mathcal{B}(B^0 \rightarrow D^{*+}D^{*-}) \times \sum \mathcal{B}(D^{*+} \rightarrow D\pi) \times \mathcal{B}(D \rightarrow X) \approx 4 \times 10^{-5}$ , is comparable to that of the  $B^0 \rightarrow J/\psi K^0$  decay mode,  $\mathcal{B}(B^0 \rightarrow J/\psi K^0) \times \sum \mathcal{B}(J/\psi \rightarrow \ell^+\ell^-) \times \mathcal{B}(K^0 \rightarrow K_S^0 \rightarrow \pi^+\pi^-) \approx 3.6 \times 10^{-5}$ . With careful optimization of the charged track reconstruction efficiency, in particular that of charged slow pions, exclusively reconstructed  $B^0 \rightarrow D^{*+}D^{*-}$  decays could permit a complementary measurement of the angle  $\beta$  of the unitarity triangle at future  $B$  factories.

In conclusion, we have fully reconstructed four  $B^0 \rightarrow D^{*+}D^{*-}$  candidates with a total estimated background of  $0.31 \pm 0.10$  events in  $5.8 \times 10^6 Y(4S) \rightarrow B\bar{B}$  decays. The probability that the estimated background could fluctuate to the observed number of signal candidate events or more is  $1.1 \times 10^{-4}$ . The branching fraction is measured to be  $\mathcal{B}(B^0 \rightarrow D^{*+}D^{*-}) = [6.2_{-2.9}^{+4.0}(\text{stat}) \pm 1.0(\text{syst})] \times 10^{-4}$  and is in agreement with the expected rate. This rate suggests that this decay could provide an avenue for the measurement of the angle  $\beta$  of the unitarity triangle.

We gratefully acknowledge the effort of the CESR staff in providing us with excellent luminosity and running conditions and the staffs of our institutions for their superb technical support. This work was supported by the National Science Foundation, the U.S. Department of Energy, the Research Corporation, the Natural Sciences and Engineering Research Council of Canada, the A.P. Sloan Foundation, the Swiss National Science Foundation, and the Alexander von Humboldt Stiftung.

\*Permanent address: University of Cincinnati, Cincinnati, OH 45221.

†Permanent address: University of Texas, Austin, TX 78712.

‡Permanent address: Yonsei University, Seoul 120-749, Korea.

- [1] BaBar Collaboration, D. Boutigny *et al.*, Technical Design Report No. SLAC-R-95-457, 1995 (unpublished).
- [2] Belle Collaboration, M. T. Cheng *et al.*, Letter of Intent, KEK Report No. 94-2, 1994 (unpublished).
- [3] Particle Data Group, C. Caso *et al.*, Eur. Phys. J. C **3**, 1 (1998).
- [4] R. Aleksan *et al.*, Phys. Lett. B **317**, 173 (1993).
- [5] I. Duniety *et al.*, Phys. Rev. D **43**, 2193 (1991).
- [6] CLEO Collaboration, D. Gibaut *et al.*, Phys. Rev. D **53**, 4734 (1996); ARGUS Collaboration, H. Albrecht *et al.*, Z. Phys. C **54**, 1 (1992).
- [7] CLEO Collaboration, D. M. Asner *et al.*, Phys. Rev. Lett. **79**, 799 (1997).
- [8] ALEPH Collaboration, R. Barate *et al.*, Eur. Phys. J. C **4**, 387 (1998).
- [9] CLEO Collaboration, Y. Kubota *et al.*, Nucl. Instrum. Methods Phys. Res., Sect. A **320**, 66 (1992).
- [10] T. Hill, Nucl. Instrum. Methods Phys. Res., Sect. A **418**, 32 (1998).
- [11] R. Brun *et al.*, GEANT3 Users Guide, CERN DD/EE/84-1.
- [12] CLEO Collaboration, M. Athanas *et al.*, Phys. Rev. Lett. **80**, 5493 (1998).
- [13] CLEO Collaboration, L. Gibbons *et al.*, Phys. Rev. D **56**, 3783 (1997).
- [14] We combine the measurements of  $(f_{+-}\tau_{B^+})/(f_{00}\tau_{B^0}) = 1.15 \pm 0.18$  and  $\tau_{B^+}/\tau_{B^0} = 1.07 \pm 0.03$  from the following two papers under the assumption that  $f_{+-} + f_{00} = 1$  to obtain  $f_{00} = 0.48 \pm 0.04$ . CLEO Collaboration, C. S. Jessop *et al.*, Phys. Rev. Lett. **79**, 4533 (1997); S. Willocq, in Proceedings of the XXIX International Conference on High Energy Physics, University of British Columbia, Vancouver, B.C., Canada, 1998 (World Scientific, Singapore, to be published); SLAC-PUB-7942.
- [15] CLEO Collaboration, M. Bishai *et al.*, CLEO Report No. CONF 97-26 (unpublished).
- [16] R. D. Cousins and V. L. Highland, Nucl. Instrum. Methods Phys. Res., Sect. A **320**, 331 (1992).